

SCIENTIFIC REPORTS

OPEN

Low-Temperature, Dry Transfer-Printing of a Patterned Graphene Monolayer

Received: 29 July 2015
Accepted: 06 November 2015
Published: 09 December 2015

Sugkyun Cha^{1,*}, Minjeong Cha^{1,*}, Seojun Lee¹, Jin Hyoun Kang² & Changsoon Kim^{1,3}

Graphene has recently attracted much interest as a material for flexible, transparent electrodes or active layers in electronic and photonic devices. However, realization of such graphene-based devices is limited due to difficulties in obtaining patterned graphene monolayers on top of materials that are degraded when exposed to a high-temperature or wet process. We demonstrate a low-temperature, dry process capable of transfer-printing a patterned graphene monolayer grown on Cu foil onto a target substrate using an elastomeric stamp. A challenge in realizing this is to obtain a high-quality graphene layer on a hydrophobic stamp made of poly(dimethylsiloxane), which is overcome by introducing two crucial modifications to the conventional wet-transfer method – the use of a support layer composed of Au and the decrease in surface tension of the liquid bath. Using this technique, patterns of a graphene monolayer were transfer-printed on poly(3,4-ethylenedioxythiophene): polystyrene sulfonate and MoO₃, both of which are easily degraded when exposed to an aqueous or aggressive patterning process. We discuss the range of application of this technique, which is currently limited by oligomer contaminants, and possible means to expand it by eliminating the contamination problem.

Graphene, a one-atom-thick layer of carbon atoms arranged in a hexagonal lattice, has outstanding electrical^{1,2} and mechanical^{3,4} properties, as well as high optical transmittance⁵. For this reason, many electronic and photonic devices employing graphene, as either an active layer or a transparent electrode, have been demonstrated, such as light-emitting diodes (LEDs)^{6,7}, solar cells^{8,9}, field-effect transistors¹⁰, photodetectors¹¹, touch screens¹², terahertz wave modulators^{13–15}, and Schottky junction devices^{16,17}. In many such demonstrations, a graphene layer has been deposited by transferring it onto a device substrate following the conventional wet-transfer method, where a graphene–polymer bilayer floating on a water bath is scooped by the substrate¹⁸. And when the patterning of graphene layers is required, it has mostly been performed after graphene transfer, typically using photolithography followed by reactive-ion etch (RIE)^{19,20}. However, this method of obtaining patterned graphene layers – the wet-transfer and subsequent patterning process – has only a limited range of applications, where graphene layers must be deposited and patterned, when necessary, prior to deposition of any material that is too fragile to withstand a wet, high-temperature, or plasma process. Notable, practically important examples of such materials are organic semiconductors²¹ and organometal trihalide perovskite compounds²².

Attention, therefore, has been focused on development of dry-transfer techniques²³. For example, a graphene layer grown on a Cu layer on a donor substrate can be directly transferred onto a target substrate, by delaminating the graphene–Cu interface when the target substrate in contact with the graphene layer is peeled off from the donor substrate²⁴. However, for selective delamination, the target substrate needs to be coated with an epoxy adhesion layer, which makes this technique unsuitable for high-performance

¹Program in Nano Science and Technology, Graduate School of Convergence Science and Technology, Seoul National University, Seoul 151-742, Republic of Korea. ²Department of Chemistry, Seoul National University, Seoul 151-747, Republic of Korea. ³Advanced Institutes of Convergence Technology, Suwon, Gyeonggi 443-270, Republic of Korea. *These authors contributed equally to this work. Correspondence and requests for materials should be addressed to C.K. (email: changsoon@snu.ac.kr)

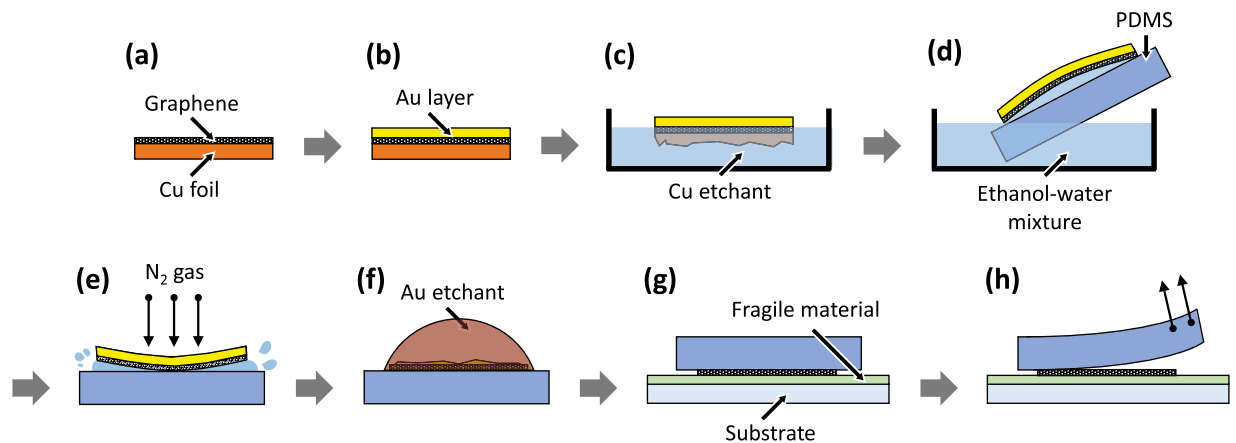


Figure 1. Transfer-printing of a CVD-grown graphene monolayer. The process begins with a graphene monolayer grown on Cu foil (a). After depositing a support layer composed of Au (b), the Cu layer is etched by floating the sample on a Cu etchant bath (c). After transferring the resulting graphene–Au bilayer to a bath comprising a mixture of water and ethanol, the bilayer was scooped up with a PDMS stamp (d). Next, the sample is blow-dried using a N₂ gun (e), followed by heat treatment on a hot plate. Removing the Au layer (f) completes the fabrication of the stamp coated with the graphene monolayer, which is then gently pressed onto a target substrate coated with a material that can be easily damaged by a wet process (g). The graphene monolayer is transferred onto the substrate as the stamp is peeled off from the substrate (h). Between (g) and (h), the stamp and substrate are kept in conformal contact for 1 h, followed by heat treatment on a hot plate.

electronic devices: for example, it cannot be applied to fabrication of an LED with a top graphene electrode, since the adhesion layer in this case would be placed in the device interior, just beneath the graphene electrode, impeding efficient charge injection. Another approach is to transfer-print a graphene layer coated with a ‘self-release’ layer from an elastomeric stamp onto a target substrate²⁵, where reliable transfer is achieved by choosing an appropriate self-release layer that assures the selective delamination at the interface between that and the elastomer. Although the transfer process itself is dry, removing the self-release layer transferred along with the graphene is typically achieved with an organic solvent, ultimately limiting applications of this method. Jung *et al.* demonstrated a technique capable of transferring graphene monolayers without an adhesion or a self-release layer²⁶. In this mechano-electro-thermal process, complete transfer, instead, requires application of high temperature ($\geq 160^\circ\text{C}$) and voltage ($\geq 600\text{ V}$) while a graphene layer grown on Cu foil is pressed onto a target substrate.

Here, we demonstrate a low-temperature, dry transfer process capable of transfer-printing a patterned graphene monolayer onto a target substrate that can be damaged or degraded by a wet, plasma or high-temperature process. In this process, a graphene monolayer on Cu foil, which is grown by chemical vapor deposition (CVD) and then patterned using a conventional lithographic process, is transferred onto a stamp made of poly(dimethylsiloxane) (PDMS), and subsequently transfer-printed from the stamp onto the target substrate. The graphene transfer from Cu foil to PDMS is achieved using the conventional wet-transfer process¹⁸, with the following two modifications: the use of Au, instead of poly(methyl methacrylate) (PMMA), as a material for the support layer, and the decrease in surface tension of the liquid bath using a water-ethanol mixture. These modifications are critical in preventing defect formation in a graphene monolayer during its transfer onto a PDMS stamp, thereby leading to a minimum sheet resistance of $573\ \Omega/\text{sq}$ for a graphene monolayer transfer-printed onto a glass substrate. Furthermore, we demonstrate transfer-printing of patterned graphene monolayers on poly(3,4-ethylenedioxythiophene): polystyrene sulfonate (PEDOT:PSS) and MoO₃, which are representative examples of organic electronic materials and practically important metal oxides²⁷, respectively, that are usually damaged or degraded when exposed to aqueous or aggressive patterning processes. The morphological and elemental characterizations of the surfaces of transfer-printed graphene show the existence of contaminants that are likely to be siloxane oligomers transferred from the PDMS stamp. We discuss the current range of application of this technique and possible means to expand it by eliminating the contamination problem.

Transfer-Printing of a Patterned Graphene Layer

To transfer a graphene monolayer onto a target substrate that can be damaged or degraded by a wet or high-temperature process (Fig. 1), we first transfer a CVD-grown graphene onto a PDMS stamp following the conventional wet-transfer method (a to f): by scooping up, with the PDMS stamp, a graphene–support bilayer floating on liquid. After the support layer is removed by chemical etching, the graphene is transfer-printed on a target substrate (g to h). The first part of this process (a to f), although seemingly

similar to the conventional wet-transfer technique¹⁸, has two distinct features, which are crucial to obtain a high-quality graphene monolayer on a target substrate.

First, as a support layer material, we use thermally deposited Au, instead of PMMA, which is most widely used for this purpose in the wet-transfer method²⁸. PDMS, the material chosen for a stamp owing to its mechanical and chemical properties suitable for various transfer-printing techniques²⁹, swells when immersed in an organic solvent³⁰ that can dissolve the PMMA support layer, such as acetone and chloroform. When this occurs, the graphene monolayer cracks, creating a large number of defects (Supplementary Fig. S1). On the contrary, the use of a Au support layer allows one to obtain a high-quality graphene monolayer on PDMS, since Au can be removed using an aqueous etchant, which does not swell PDMS.

Second, for the liquid on which the graphene–Au bilayer floats and from which it is scooped with a PDMS stamp [Fig. 1(d)], we use an ethanol–water mixture, instead of water commonly used in the conventional wet-transfer technique. This is to decrease the surface tension of the liquid. In the conventional case, after the graphene–support bilayer is scooped with a hydrophilic substrate [as in Fig. 1(d)], a thin layer of water is present throughout the graphene–substrate interface, providing sufficient lubrication at that interface. As a result, when the sample is blow-dried using a N₂ gun, the graphene and substrate form a conformal contact without wrinkles throughout the substrate, as the water is laterally displaced [Supplementary Fig. S2(a)]. Since the surface of a PDMS stamp is hydrophobic, which is favorable for reliable transfer of a graphene monolayer onto a target substrate via stamping (g to h in Fig. 1), the use of water bath in Fig. 1(d) leads to a discontinuous lubrication layer between the bilayer and substrate, as schematically shown in Supplementary Fig. S2(b). Therefore, blow-drying in this case results into bursting of trapped water droplets, tearing the graphene monolayer. This can be effectively prevented by using an ethanol–water mixture as the liquid bath, which sufficiently wets the PDMS surface to provide a continuous lubrication layer [Supplementary Fig. S2(c)].

When patterning of graphene is required, a conventional patterning process, such as O₂ RIE of graphene using photoresist patterned by photolithography as an etch mask^{19,20}, is performed before Step (b) in Fig. 1. Then, performing the remaining processes [Step (b) to (h)], one can obtain a patterned graphene monolayer on a target substrate. This pre-transfer patterning of graphene allows one to avoid possible damage to the fragile material that is likely to occur, when a process such as photolithography^{19,20}, RIE^{19,20}, or laser ablation³¹ is performed after the graphene is transferred to the target substrate.

Results and Discussion

To show that the surface tension of a liquid used in Step (d) in Fig. 1 is a critical factor determining the quality of transfer-printed graphene, we transfer-printed a graphene monolayer on a Si substrate coated with a 285-nm-thick SiO₂ layer following a process described in Fig. 1, while varying the liquid bath: in one set of experiments, we used water, and in the other, a water–ethanol mixture (30% water and 70% ethanol by volume). When water bath was used, although the entire graphene sheet (1.3 cm by 1.3 cm) was seemingly well-transferred, a closer observation revealed that there are randomly distributed irregular-shaped holes where graphene is absent, as shown in Fig. 2(a). The density of these defects is approximately 10 cm⁻², which was obtained by counting the number of defects distributed over the whole sample area using an optical microscope. When the PDMS stamp was observed by an optical microscope after Step (f) in Fig. 1, it was found that similar defects, albeit smaller in size, were present (Supplementary Fig. S3), indicating that the defects are formed while transferring the graphene layer onto the PDMS surface and are exacerbated during the transfer-printing onto the substrate. As described in the previous section, the defects arise from insufficient wetting of the PDMS surface by water. Since PDMS is hydrophobic and water has high surface tension (≈ 72 dyn/cm at 23 °C), immediately after a graphene–Au bilayer is scooped by a PDMS stamp, water dewets the PDMS surface in several locations, making the bilayer form contacts to the PDMS surface that is only locally conformal [Supplementary Figs S2(b) and S4(a)]. As the sample is blow-dried using a N₂ gun, these locally conformal contacts laterally expand, generating narrow wrinkles with water droplets trapped inside, as shown in the right image of Supplementary Fig. S4(a). We speculate that further application of N₂ pressure causes the water droplets to burst, resulting into defects such as that shown in Supplementary Fig. S3. In fact, as shown in Fig. 2(a), the locations of many defects in the graphene transferred onto the substrate seem to coincide with the intersection of the wrinkles, where relatively large water droplets are expected to form: the linear regions in Fig. 2(a) indicated by the white arrow are where the graphene monolayer is folded, which results from the wrinkles in the graphene–Au bilayer. In contrast, when the ethanol–water mixture was used, its lower surface tension (≈ 25 dyn/cm at 23 °C³²) allows a continuous lubrication layer to form between the graphene and PDMS surfaces, providing effective “decoupling” of the bilayer from the PDMS surface. Therefore, no wrinkles, except a few with much smaller heights, were observed in the graphene–Au bilayer on the PDMS stamp [Supplementary Fig. S4(b)]. We found that mild baking at 40 °C removes these wrinkles, resulting into the flat graphene–Au bilayer that is globally conformal to the PDMS stamp, and consequently, successful transfer-printing of the graphene monolayer was achieved without defects, as shown in Fig. 2(b).

The sheet resistance (R_{sh}) was measured for graphene monolayers transfer-printed on glass substrates, using the van der Pauw method³³. The size of the graphene monolayers are approximately 1.3 cm by 1.3 cm, and the R_{sh} values were obtained with an injected current of 1 mA. In the following, a graphene

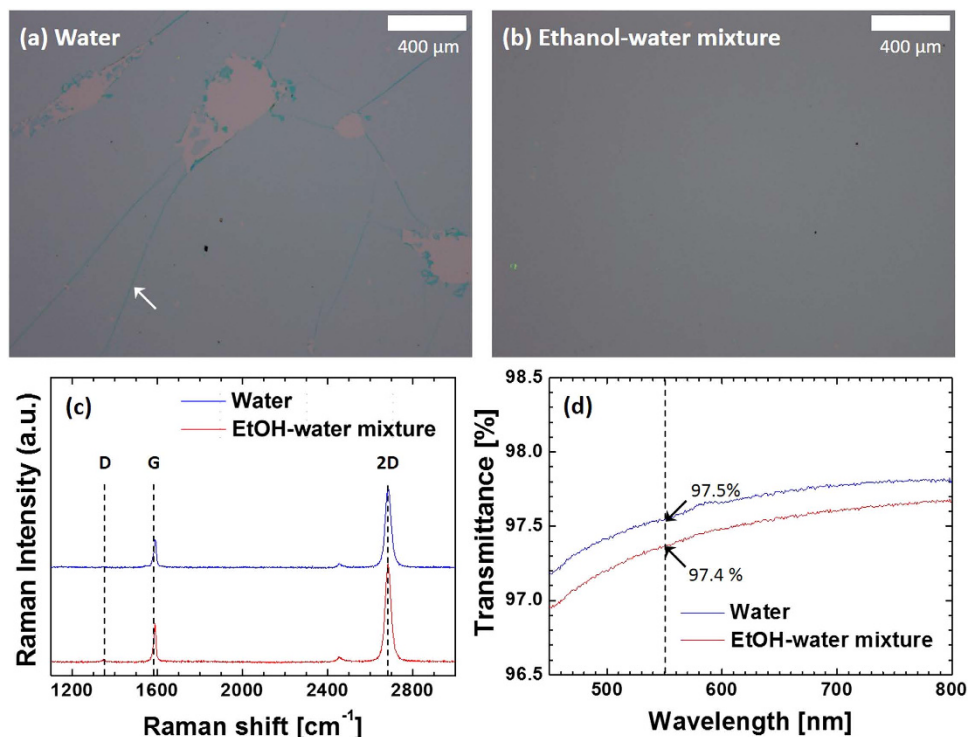


Figure 2. Effect of surface tension on the quality of transfer-printed graphene monolayers. (a,b) Optical microscope images of graphene monolayers transfer-printed on Si substrates pre-coated with SiO₂. The bath used in step (d) in Fig. 1 is composed of water in (a) and a water–ethanol mixture in (b). Along a line indicated by the arrow in (a), the graphene monolayer is folded, which arises from a corresponding wrinkle in the graphene–Au bilayer formed due to insufficient wetting of the PDMS surface by the bilayer. (c) Raman spectra of the graphene monolayers on the Si/SiO₂ substrates. (d) Optical transmittance spectra of the graphene monolayers transferred on glass substrates. Each curve was obtained by averaging over five samples.

monolayer transfer-printed onto a final substrate from a PDMS stamp onto which a graphene–Au bilayer was scooped from a bath of water and the ethanol–water mixture are referred to as $G_{\text{H}_2\text{O}}$ and $G_{\text{EtOH-H}_2\text{O}}$ respectively. For $G_{\text{H}_2\text{O}}$, the sheet resistance, averaged over five samples ($\langle R_{\text{sh}} \rangle$) is 3119 Ω/sq , with a minimum equal to 2664 Ω/sq . In contrast, for $G_{\text{EtOH-H}_2\text{O}}$, $\langle R_{\text{sh}} \rangle$ is 914 Ω/sq , with a minimum being 573 Ω/sq . Figure 2(c) shows Raman spectra of graphene monolayers shown in Fig. 2(a,b), where for $G_{\text{H}_2\text{O}}$ they were obtained from defect-free regions. The spectra show that, for both cases, (i) each Raman peak occurs at the same location (D: 1344 cm^{-1} , 2D: 2686 cm^{-1} , G: 1588 cm^{-1}), (ii) the height of the D peaks is negligible, and (iii) the 2D/G peak ratios are larger than 2.7, confirming that the transfer-printed graphene is indeed a monolayer³⁴. This result indicates that significantly larger values of R_{sh} for $G_{\text{H}_2\text{O}}$, in comparison to that for $G_{\text{EtOH-H}_2\text{O}}$, are due not to the properties of graphene in defect-free regions, but to large-scale defects as shown in Fig. 2(a), which has been prevented by decreasing the surface tension in the case of $G_{\text{EtOH-H}_2\text{O}}$. Electrical doping of graphene by ethanol may have occurred for $G_{\text{EtOH-H}_2\text{O}}$ and contributed to the decrease in R_{sh} , which has been ruled out by an experiment described in Note 1 in Supplementary Material.

Figure 2(d) shows the optical transmission spectra of $G_{\text{H}_2\text{O}}$ and $G_{\text{EtOH-H}_2\text{O}}$ transfer-printed on a 0.7-mm-thick glass substrate, averaged over five samples for each case. Transmittance (T), plotted on the y -axis, is the intensity of the optical beam transmitted through a glass/graphene sample normalized to that transmitted through a glass substrate. The size of the optical beam at the sample location was approximately 2 mm by 8 mm. For both $G_{\text{H}_2\text{O}}$ and $G_{\text{EtOH-H}_2\text{O}}$, the values of T are consistent with what was previously measured for a graphene monolayer on a quartz substrate¹². The value of T for $G_{\text{H}_2\text{O}}$ is slightly higher than that for $G_{\text{EtOH-H}_2\text{O}}$, primarily because the absence of graphene in the defects in $G_{\text{H}_2\text{O}}$ allow more light to be transmitted. Under this hypothesis, the ratio of total area of the defects to the entire area of the graphene sheet (α) can be estimated as $\alpha = (T_{\text{H}_2\text{O}} - T_{\text{EtOH-H}_2\text{O}})/(1 - T_{\text{EtOH-H}_2\text{O}})$, where $T_{\text{H}_2\text{O}}$ and $T_{\text{EtOH-H}_2\text{O}}$ are transmittance of $G_{\text{H}_2\text{O}}$ and $G_{\text{EtOH-H}_2\text{O}}$, respectively. The value of α

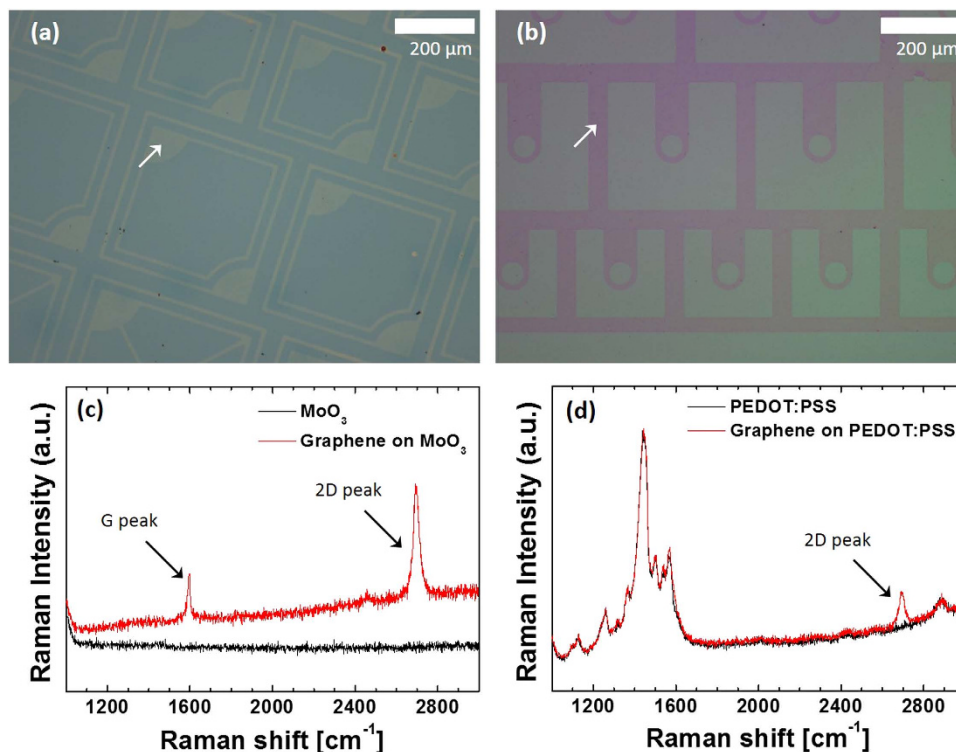


Figure 3. Characterizations of graphene monolayer patterns transfer-printed on materials that can be damaged by a wet process. (a,b) Optical microscope images of graphene monolayer patterns transfer-printed on (a) MoO₃ and (b) PEDOT:PSS. The arrows in (a,b) indicate regions covered by graphene monolayers. (c,d) Raman spectra (red) of the patterned graphene on (c) MoO₃ and (d) PEDOT:PSS. Also shown are the Raman spectra of the substrates without graphene (black).

calculated at each wavelength in Fig. 2(d) ranges from 6% to 8%, which is consistent with our estimation based on optical microscope images.

As expected, successful transfer-printing of graphene requires a defect-free graphene monolayer that is globally conformal to a PDMS stamp. Our proposed technique achieves this with the water-ethanol mixture, which provides a continuous lubrication layer, and with a Au support layer, which allows for its removal without swelling PDMS. Alternatively, one may attempt to obtain a defect-free graphene monolayer on a PDMS stamp by pressing the stamp onto a graphene layer grown on Cu foil and then etching away the Cu foil by floating the Cu/graphene/PDMS on a bath of a Cu etchant. Since the surface of Cu foil commonly used in CVD growth of graphene typically has corrugations on the micron scale²⁸, the PDMS attached to the graphene in this case is in contact with the graphene only partially. As a result, subsequent processes such as N₂ blow-dry and transfer-printing tend to cause defects in the graphene layer, as shown in Supplementary Fig. S5. In fact, it was previously reported that R_{sh} of a transfer-printed graphene monolayer by this approach was 4 k Ω /sq, even with a self-release layer inserted for reliable graphene transfer²⁵.

To fabricate practical electronic devices where graphene is used as active layers or electrodes, the patterning of graphene is required. Our technique, described in Fig. 1, can achieve this with a simple modification: the process begins with a patterned graphene on Cu foil in Step (a), instead of an unpatterned graphene layer. In our current demonstration, we first prepared a patterned graphene monolayer on Cu foil by etching unpatterned graphene grown on Cu foil by O₂ RIE using a photoresist etch mask patterned by photolithography. Next, the patterned graphene was transfer-printed on a Si/SiO₂ substrate coated with MoO₃ or PEDOT:PSS, both of which are susceptible to degradation when exposed to an aqueous condition or aggressive patterning process. Figure 3(a,b) are optical micrographs of the substrates, where patterned graphene monolayers were transfer-printed in regions indicated by the arrows, showing that the patterns defined on photomasks were replicated in the transfer-printed graphene monolayers. The widths of the smallest features – lines in Fig. 3(a) and arcs in Fig. 3(b) – are 10 μ m and 15 μ m, respectively, which are identical, within the resolution of the optical imaging system used (\sim 0.5 μ m), to those of the corresponding features on the photomask. A closer observation of the pattern edge using a field emission scanning electron microscope (FE-SEM) revealed that it is not straight on the nanoscale, with an “edge resolution” of 50 nm, which is probably attributed to the edge resolution of the photomask patterns and/or limitation of the photolithography process (Supplementary Fig. S7). From this, together with the fact that previously demonstrated transfer-printing-based patterning techniques can

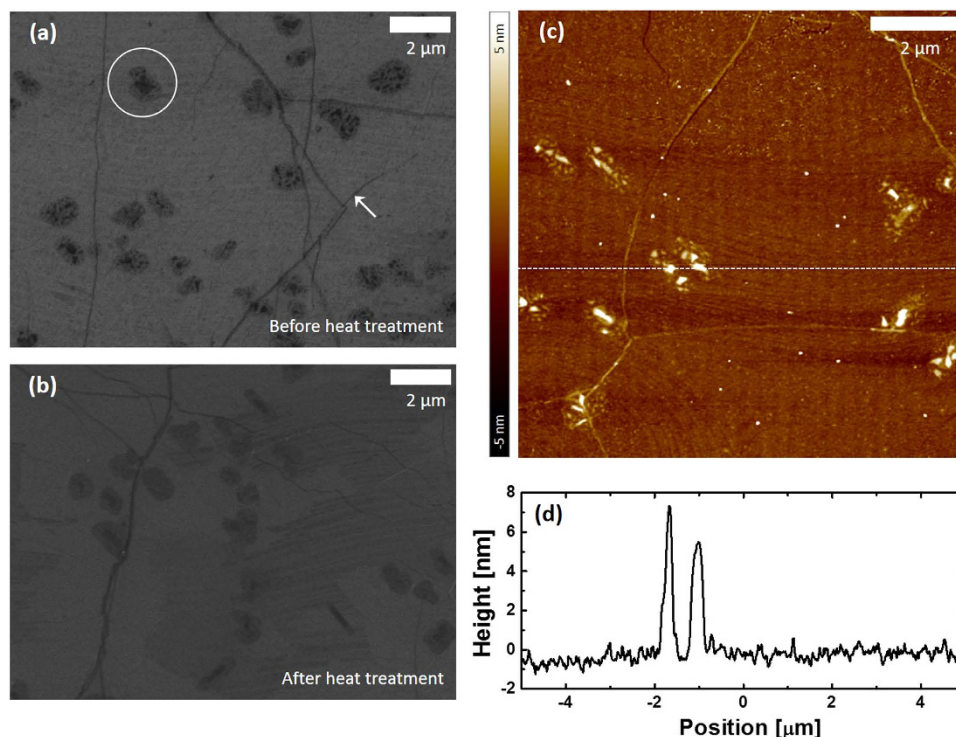


Figure 4. Morphological characterizations of transfer-printed graphene monolayers. (a,b) Scanning electron microscope images of the graphene surface before (a) and after (b) annealing at 400 °C under H₂ and Ar. (c) Atomic force microscope image of the sample used in (a). (d) Height profile of the surface measured along the white dotted line in (c).

create patterns whose size is well below 100 nm³⁵, we expect that our technique is capable of creating sub-micrometer graphene patterns, if a nanopatterning process, for example electron-beam³⁶, nanoimprint³⁷, or nanosphere³⁸ lithography, is employed, instead of photolithography. Raman spectra obtained from the graphene transfer-printed on the MoO₃ show the distinct G and 2D peaks, with the 2D/G intensity ratio of 2.5, and the negligible D peak, suggesting that the quality of the graphene is comparable to that in Fig. 2(b). For the case of the graphene transfer-printed onto the PEDOT:PSS, the peaks associated with graphene, except the 2D peak, cannot be identified due to the overlap with Raman spectra of PEDOT:PSS.

Next, we observed the surface of the transfer-printed graphene on a Si/SiO₂ substrate, using a FE-SEM and an atomic force microscope (AFM). As shown in Fig. 4(a), irregularly shaped dark patches, as enclosed by a white circle, are randomly distributed throughout the surface. Also shown are the dark lines, as marked by the white arrow. These two features, patches and lines, are commonly found in the transferred graphene CVD-grown on Cu foil – with the former and latter attributed to graphene multilayers and wrinkles, respectively²⁸ – and hence are not caused by our transfer technique. It is also shown that in the patches, there are darker spots with diameters of approximately 150 nm. The surface profile measured using an AFM along the white dotted line in Fig. 4(c) shows that the spots have heights as high as approximately 7 nm [Fig. 4(d)]. To identify the origin of the dark spots, elemental analysis was carried out using a scanning transmission electron microscope capable of energy dispersive x-ray spectroscopy (STEM-EDS). In order to prepare a sample for this analysis, a graphene layer was transfer-printed from a PDMS stamp onto a Si/SiO₂ substrate coated with a PEDOT:PSS separation layer, and then transferred onto a lacey carbon TEM grid using the conventional wet-transfer method (see the Method Section for the experimental detail). An EDS spectrum obtained from a region shown in Supplementary Fig. S8(a) shows that, in addition to carbon, silicon atoms are present on the graphene surface [Supplementary Fig. S8(b)]. Given many previous reports showing that uncured siloxane oligomers were present on PDMS surfaces^{25,39}, it is highly likely that the dark spots on the graphene surface are siloxane residues that have been transferred from the PDMS stamp. This speculation was further supported by the fact that the dark spots can be eliminated by annealing the sample at 400 °C under H₂ and Ar, as shown in Fig. 4(b)⁴⁰. The AFM measurements [Fig. 4(c,d)] show that the surface in the background, that is, regions away from the patches and lines, is much rougher than that of a clean graphene surface⁴¹, suggesting that the oligomer residues are also present throughout the surface, not only on the multilayer regions.

The morphological and elemental characterizations of the surface of transfer-printed graphene discussed above help determine the range of application of our technique in its current form. Since the

oligomer residues are likely to be present only on the top surface, that is, the graphene surface that used to be in contact with the PDMS, our technique can be applied to fabrication of (i) devices where only the bottom surface of the graphene electrode is involved in injection or collection of charge carriers, such as LEDs and solar cells, made of organic semiconductors⁴² or organometal trihalide perovskite compounds⁴³, with top graphene electrodes, and (ii) devices whose graphene electrodes are used to establish electric fields without charge carrier transport, such as thin-film transistors with graphene gate electrodes⁴⁴ and terahertz wave modulators^{13–15}. Meanwhile, when charge carrier injection or collection occurs in both sides of the graphene layer, such as in tandem LEDs and solar cells where it is part of the interlayers, our technique is not applicable. Therefore, expanding the range of application of our technique by eliminating the oligomer contamination, possibly with the following modification, is important future work: replacing PDMS with other stamp material that can be completely cured; or depositing a blocking layer on the PDMS surface to prevent possible transfer of uncured oligomers onto the graphene surface, with a potential candidate being a pressure sensitive adhesive layer^{45,46}.

A possible concern with choosing Au as a material for the support layer is its high cost. Although Au is an expensive material, the thinness of the support layer translates to a small amount of Au used per area: the 200-nm-thick Au support layer corresponds to 0.386 mg of Au per cm², whose cost may not be of a concern for many device applications. Another concern may be effects of the Au etchant on the electrical quality of transfer-printed graphene. In our experiments, exposure of graphene to the Au etchant is rather brief (<5 min), after which samples are thoroughly rinsed with clean water. As a result, the elemental characterization of the transfer-printed graphene layer in Fig. S8 does not show any peaks associated with the Au etchant, such as those of iodine. Furthermore, through a simple experiment described in Note 2 in Supplementary Material, we have confirmed that the change in R_{sh} due to the Au etchant is negligible. Finally, we note that Au in our demonstration can be considered as a representative material for the support layer satisfying the following conditions — it must not be etched away by the Cu etchant, and can be removed without swelling PDMS and damaging graphene — and hence can be replaced by other material, not necessarily metallic, that is more cost-effective and/or easily removed.

Conclusion

In summary, we have developed a low temperature, dry process capable of transfer-printing a patterned graphene monolayer grown on Cu foil on a target substrate. Two features distinct from the conventional wet-transfer method¹⁸ — the use of a support layer composed of Au, instead of PMMA, and the decrease in surface tension of the liquid bath on which a graphene–Au bilayer floats — allow one to obtain a graphene monolayer on a PDMS stamp without defects that would otherwise arise. Subsequently, the graphene is transfer-printed from the stamp onto a target substrate. The characteristics of a graphene monolayer transfer-printed using our technique are comparable to those obtained with the conventional wet-transfer method, with a sheet resistance as low as 573 Ω /sq and optical transmittance of 97.4% at 550 nm. In addition, with pre-transfer patterning of graphene on Cu foil using conventional patterning processes, our technique is capable of creating graphene monolayer patterns on materials that are easily degraded when exposed to high-temperature processes, organic solvents, or aqueous chemicals. As an example, using photolithography followed by reactive-ion etch to pattern graphene monolayers on Cu foil and then transfer-printing them, we have obtained graphene monolayer patterns on MoO₃ and PEDOT:PSS, with the smallest feature size and edge resolution of $\approx 10 \mu\text{m}$ and 50 nm, respectively. Immediate application areas of this technique include organic electronic devices whose top electrodes are composed of graphene. Moreover, by eliminating siloxane oligomer residues on graphene using alternate stamp material, the technique can be further applied to devices whose graphene electrodes are in their interiors, such as tandem LEDs and solar cells. Finally, with possible appropriate modification, it may also be applied to dry-transfer of other two-dimensional materials, including boron nitride⁴⁷ and molybdenum disulfide⁴⁸.

Methods

CVD-grown graphene monolayer. A graphene monolayer on Cu foil was grown in a CVD system consisting of a tubular quartz reactor and a furnace. Experimental details described in ref. 12 were closely followed except the following: Cu foil was annealed under a 5 sccm flow of H₂ at 20 mTorr, and during growth, the reactor was filled with a mixture of CH₄ and H₂ at a total pressure of 150 mTorr, whose flow rates are 35 and 5 sccm, respectively.

Low-temperature, dry transfer-printing process. Low-temperature, dry transfer of graphene monolayers was carried out by following processes described in Fig. 1. To form a support layer on a graphene monolayer on Cu foil, a 200-nm-thick Au layer was deposited by thermal evaporation in high vacuum (1 \AA /s, $\sim 10^{-7}$ Torr) (b). To etch away the Cu foil, the Cu/graphene/Au multilayer was floated on an ammonium persulfate solution, prepared by dissolving 10 g of ammonium persulfate (Sigma Aldrich) in 500 ml of water (c). After the etch was completed, the graphene–Au bilayer was scooped with a glass slide, and then transferred on a bath of water to remove residual ammonium persulfate. Next, the graphene–Au bilayer was moved onto a bath composed of an ethanol–water mixture (70 vol % ethanol and 30 vol % water), from which the bilayer was scooped by and transferred onto a PDMS stamp (d). The sample was then blow-dried using a N₂ gun (e), and was further dried on a hot plate at 40 °C for

more than 4 h. The Au support layer was etched using an ammonium iodide solution (LAE-202, Cowon Innotech. Inc.) (f), after which the PDMS/graphene sample was rinsed with water. After water droplets on the sample were blown away using a N₂ gun, the graphene-coated PDMS stamp was gently pressed onto a target substrate, inducing intimate contact throughout the substrate area (g). Before separation of the stamp from the substrate, the sample was stored at room temperature for 1 h under a pressure of 9.9 kPa, and then placed on a hot plate at 70 °C for 10 min without application of pressure. Finally, the stamp was carefully peeled off from the substrate (h), resulting in the transfer-printed graphene monolayer on the target substrate.

Transfer-printing of patterned graphene layers. In this process, a graphene monolayer on Cu foil was first patterned using conventional photolithography and reactive-ion etch, as described in Supplementary Fig. S6. A 1.5- μm -thick photoresist (AZ GXR-601, 14cP) was spin-coated on a Cu/graphene sample, and then patterned by photolithography. The patterned graphene on Cu foil was obtained, when the graphene in the areas not covered by the photoresist was etched by reactive ion etch in O₂ (100 W, 0.1 Torr, 20 s, 50 sccm). Performing the processes described in Fig. 1 with this sample, instead of unpatterned graphene on Cu foil, we transfer-printed a patterned graphene monolayer on a target substrate coated with a 75-nm-thick PEDOT:PSS or a 20-nm MoO₃ layer. The target substrate was a 500- μm -thick Si substrate pre-coated with a 285-nm-thick thermal SiO₂ layer, and the PEDOT:PSS (Heraeus) and MoO₃ (LTS Chemical Inc.) layers were deposited by spin-coating (3000 rpm, 30 s) and thermal evaporation in high vacuum (1 Å/s, $\sim 10^{-7}$ Torr), respectively.

Sample preparation for the elemental analysis. Samples for the elemental analysis were prepared following the processes described in Supplementary Fig. S9. After a graphene monolayer was transfer-printed from a PDMS stamp onto a PEDOT:PSS layer using our transfer method (a), a layer of PMMA was deposited on the graphene layer by spin coating at 3000 rpm for 30 s (b). The PMMA solution was prepared by dissolving PMMA (138 mg, Sigma Aldrich) into chlorobenzene (3 mL, Sigma Aldrich). The sample was then immersed into a water bath, separating the PMMA-graphene bilayer from the Si/SiO₂ substrate as the PEDOT:PSS layer was dissolved (c). Next, the bilayer was transferred to another water bath and kept floating on it for more than 24 h to ensure that PEDOT:PSS remaining on the graphene surface was removed. Then, the bilayer was scooped with a lacey carbon TEM grid (Ted Pella, Inc.) (d), after which the grid was placed on a hot plate at 40 °C for more than 2 h. Finally, the PMMA layer was removed by acetone (e), resulting in the graphene monolayer on the TEM grid (f).

Characterization of transfer-printed graphene layers. The surface morphology of transfer-printed graphene layers was characterized using a FE-SEM (JSM-6700F, JEOL) and an AFM (Dimension Edge, Bruker). The sheet resistance was measured using a source meter (2400, Keithley) and a multimeter (34410A, Agilent). The Raman spectra were obtained using a confocal Raman microscope (inVia, Renishaw) with an excitation wavelength of 514.5 nm emitted from an Ar laser. An ultraviolet-visible spectrophotometer (Lambda 35, Perkin Elmer) was used to measure the optical transmittance spectra. The elemental analysis was carried out using a STEM equipped with an EDS (JEM-2100F, JEOL).

References

- Novoselov, K. S. *et al.* Electric field effect in atomically thin carbon films. *Science* **306**, 666–669 (2004).
- Castro Neto, A. H., Guinea, F., Peres, N. M. R., Novoselov, K. S. & Geim, A. K. The electronic properties of graphene. *Rev. Mod. Phys.* **81**, 109–162 (2009).
- Liu, F., Ming, P. & Li, J. Ab initio calculation of ideal strength and phonon instability of graphene under tension. *Phys. Rev. B* **76**, 064120-1–064120-7 (2007).
- Lee, C., Wei, X., Kysar, J. W. & Hone, J. Measurement of the elastic properties and intrinsic strength of monolayer graphene. *Science* **321**, 385–388 (2008).
- Nair, R. R. *et al.* Fine structure constant defines visual transparency of graphene. *Science* **320**, 1308 (2008).
- Meyer, J. *et al.* Metal oxide induced charge transfer doping and band alignment of graphene electrodes for efficient organic light emitting diodes. *Sci. Rep.* **4**, 5380–5386 (2014).
- Kim, B. J. *et al.* Large-area transparent conductive few-layer graphene electrode in GaN-based ultra-violet light-emitting diodes. *Appl. Phys. Lett.* **99**, 143101-1–143101-3 (2011).
- Wang, Y., Tong, S. W., Xu, X. F., Özyilmaz, B. & Loh, K. P. Interface engineering of layer-by-layer stacked graphene anodes for high-performance organic solar cells. *Adv. Mater.* **23**, 1514–1518 (2011).
- Park, H., Brown, P. R., Bulović, V. & Kong, J. Graphene as transparent conducting electrodes in organic photovoltaics: studies in graphene morphology, hole transporting layers, and counter electrodes. *Nano Lett.* **12**, 133–140 (2012).
- Di, C. *et al.* Patterned graphene as source/drain electrodes for bottom-contact organic field-effect transistors. *Adv. Mater.* **20**, 3289–3293 (2008).
- Baierl, D., Fabel, B., Lugli, P. & Scarpa, G. Efficient indium-tin-oxide (ITO) free top-absorbing organic photodetector with highly transparent polymer top electrode. *Org. Electron.* **12**, 1669–1673 (2011).
- Bae, S. *et al.* Roll-to-roll production of 30-inch graphene films for transparent electrodes. *Nat. Nanotechnol.* **5**, 574–578 (2010).
- Sensale-Rodriguez, B. *et al.* Broadband graphene terahertz modulators enabled by intraband transitions. *Nat. Commun.* **3**, 780–786 (2012).
- Gao, W. *et al.* High-contrast terahertz wave modulation by gated graphene enhanced by extraordinary transmission through ring apertures. *Nano Lett.* **14**, 1242–1248 (2014).
- Li, Q. *et al.* Active graphene-silicon hybrid diode for terahertz waves. *Nat. Commun.* **6**, 7082–7087 (2015).
- Yang, H. *et al.* Graphene barristor, a triode device with a gate-controlled Schottky barrier. *Science* **336**, 1140–1143 (2012).

17. Tongay, S. *et al.* Rectification at graphene-semiconductor interfaces: zero-gap semiconductor-based diodes. *Phys. Rev. X* **2**, 011002-1–011002-10 (2012).
18. Li, X. *et al.* Large-area synthesis of high-quality and uniform graphene films on copper foils. *Science* **324**, 1312–1314 (2009).
19. Lee, W. H. *et al.* Transparent flexible organic transistors based on monolayer graphene electrodes on plastic. *Adv. Mater.* **23**, 1752–1756 (2011).
20. Shi, R., Xu, H., Chen, B., Zhang, Z. & Peng, L. M. Scalable fabrication of graphene devices through photolithography. *Appl. Phys. Lett.* **102**, 113102-1–113102-5 (2013).
21. Forrest, S. R. The path to ubiquitous and low-cost organic electronic appliances on plastic. *Nature* **428**, 911–918 (2004).
22. Snath, H. J. Perovskites: The emergence of a new era for low-cost, high-efficiency solar cells. *J. Phys. Chem. Lett.* **4**, 3623–3630 (2013).
23. Kang, J., Shin, D., Bae S. & Hong B. H. Graphene transfer: key for applications. *Nanoscale* **4**, 5527–5537 (2012).
24. Yoon, T. *et al.* Direct measurement of adhesion energy of monolayer graphene as-grown on copper and its application to renewable transfer process. *Nano Lett.* **12**, 1448–1452 (2012).
25. Song, J. *et al.* A general method for transferring graphene onto soft surfaces. *Nat. Nanotechnol.* **8**, 356–362 (2013).
26. Jung, W. *et al.* Ultraconformal contact transfer of monolayer graphene on metal to various substrates. *Adv. Mater.* **26**, 6394–6400 (2014).
27. Giroto, C., Voroshazi, E., Cheyns, Heremans, P. & Rand, B. P. Solution-processed MoO₃ thin films as a hole-injection layer for organic solar cells. *ACS Appl. Mater. Interfaces* **3**, 3244–3247 (2011).
28. Li, X. *et al.* Transfer of large-area graphene films for high-performance transparent conductive electrodes. *Nano Lett.* **9**, 4359–4363 (2009).
29. Xia, Y. & Whitesides, G. M. Soft lithography. *Angew. Chem. Int. Ed.* **37**, 550–575 (1998).
30. Lee, J. N., Park, C. & Whitesides, G. M. Solvent compatibility of poly(dimethylsiloxane)-based microfluidic devices. *Anal. Chem.* **75**, 6544–6554 (2003).
31. Kalita, G., Qi, L., Namba, Y., Wakita, K. & Umeno M. Femtosecond laser induced micropatterning of graphene film. *Mater. Lett.* **65**, 1569–1572 (2011).
32. Hansen C. New simple method to measure polymer surface tension. *Pigm. Resin Technol.* **27**, 374–378 (1998).
33. van der Pauw, L. J. A method of measuring specific resistivity and Hall effect of discs of arbitrary shape. *Philips Tech. Rev.* **13**, 1–9 (1958).
34. Ferrari, A. C. *et al.* Raman spectrum of graphene and graphene layers. *Phys. Rev. Lett.* **97**, 187401-1–187401-4 (2006).
35. Kim, C., Shtein, M. & Forrest, S. R. Nanolithography based on patterned metal transfer and its application to organic electronic devices. *Appl. Phys. Lett.* **80**, 4051–4053 (2002).
36. Withers, F., Bointon, T. H., Dubois, M., Russo, S. & Craciun M. F. Nanopatterning of fluorinated graphene by electron beam irradiation. *Nano Lett.* **11**, 3912–3916 (2011).
37. Liang, X. *et al.* Formation of bandgap and subbands in graphene nanomeshes with sub-10 nm ribbon width fabricated via nanoimprint lithography. *Nano Lett.* **10**, 2454–2460 (2010).
38. Liu, L. *et al.* Nanosphere lithography for the fabrication of ultranarrow graphene nanoribbons and on-chip bandgap tuning of graphene. *Adv. Mater.* **23**, 1246–1251 (2011).
39. Glasmästar, K., Gold, J., Andersson, A.-S., Sutherland, D. S. & Kasemo, B. Silicone transfer during microcontact printing. *Langmuir* **19**, 5475–5483 (2003).
40. Allen, M. J. *et al.* Soft transfer printing of chemically converted graphene. *Adv. Mater.* **21**, 2098–2102 (2009).
41. Pirkle, A. *et al.* The effect of chemical residues on the physical and electrical properties of chemical vapor deposited graphene transferred to SiO₂. *Appl. Phys. Lett.* **99**, 122108-1–122108-3 (2011).
42. Beck, J. H. *et al.* Clean graphene electrodes on organic thin-film devices via orthogonal fluorinated chemistry. *Nano Lett.* **15**, 2555–2561 (2015).
43. You, P., Liu, Z., Tai, Q., Liu, S. & Yan, F. Efficient semitransparent perovskite solar cells with graphene electrodes. *Adv. Mater.* **27**, 3632–3638 (2015).
44. Park, J. K., Song, S. M., Mun, J. H. & Cho, B. J. Graphene gate electrode for MOS structure-based electronic devices. *Nano Lett.* **11**, 5383–5386 (2011).
45. Choi, T. *et al.* Roll-to-roll continuous patterning and transfer of graphene via dispersive adhesion. *Nanoscale* **7**, 7138–7142 (2015).
46. Kim, S. J. *et al.* Ultraclean patterned transfer of single-layer graphene by recyclable pressure sensitive adhesive films. *Nano Lett.* **15**, 3236–3240 (2015).
47. Zhang, C. *et al.* Direct growth of large-area graphene and boron nitride heterostructures by a co-segregation method. *Nat. Commun.* **6**, 6519–6526 (2015).
48. Shi, Y. *et al.* van der Waals epitaxy of MoS₂ layers using graphene as growth templates. *Nano Lett.* **12**, 2784–2791 (2012).

Acknowledgements

This work was supported by the Global Frontier R&D Program on the Center for Multiscale Energy System (Grant No. 2011-0031561) and the Center for THz-Bio Application Systems (Grant No. 2009-0083512)–both by the National Research Foundation under the Ministry of Science, ICT, and Future Planning, Korea– and by the 2015 Promising-Pioneering Researcher Program of Seoul National University.

Author Contributions

M.C. and C.K. conceived the main idea of the transfer-printing process, and designed the experiments; S.C. performed CVD-growth of graphene used in all experiments, prepared and characterized graphene patterns on MoO₃ and PEDOT:PSS, and performed AFM and FE-SEM measurements, and elemental characterization; S.C. and M.C. carried out the remaining experiments, except the acquisition of the Raman spectra, which was performed by J.H.K.; S.C., M.C. and C.K. analyzed the data; C.K., S.C. and S.L. wrote the manuscript.

Additional Information

Supplementary information accompanies this paper at <http://www.nature.com/srep>

Competing financial interests: The authors declare no competing financial interests.

How to cite this article: Cha, S. *et al.* Low-Temperature, Dry Transfer-Printing of a Patterned Graphene Monolayer. *Sci. Rep.* **5**, 17877; doi: 10.1038/srep17877 (2015).



This work is licensed under a Creative Commons Attribution 4.0 International License. The images or other third party material in this article are included in the article's Creative Commons license, unless indicated otherwise in the credit line; if the material is not included under the Creative Commons license, users will need to obtain permission from the license holder to reproduce the material. To view a copy of this license, visit <http://creativecommons.org/licenses/by/4.0/>